Research Square

Preprints are preliminary reports that have not undergone peer review.
They should not be considered conclusive, used to inform clinical practice,
or referenced by the media as validated information.

Thermomechanical Simulation of Friction Stir Welding in Dissimilar Materials: A Comprehensive Review and Numerical Investigation for Aluminum Polymer Joint

Khamda Herbandono

kham001@brin.go.id

National Research and Innovation Agency https://orcid.org/0009-0002-8600-4354

Harry Purnama

National Research and Innovation Agency https://orcid.org/0000-0003-1844-5529

Dede Santoso

National Research and Innovation Agency https://orcid.org/0009-0001-5826-5218

Katri Yulianto

National Research and Innovation Agency https://orcid.org/0009-0000-6663-5648

Systematic Review

Keywords: numerical simulation, friction stir welding, dissimilar material, lightweight components

Posted Date: August 4th, 2026

DOI: https://doi.org/10.21203/rs.3.rs-10558670/v1

License: This work is licensed under a Creative Commons Attribution 4.0 International License.
Read Full License

Additional Declarations: The authors declare no competing interests.

(Article)

Thermomechanical Simulation of Friction Stir Welding in Dissimilar Materials: A Comprehensive Review and Numerical Investigation for Aluminum Polymer Joint

Khamda Herbandono[1,2,*], (kham001@brin.go.id), https://orcid.org/0009-0002-8600-4354
Harry Purnama[1], (harr007@brin.go.id), https://orcid.org/0000-0003-1844-5529
Dede Santoso[1], (dede026@brin.go.id), https://orcid.org/0009-0001-5826-5218
Katri Yulianto[1], (katr001@brin.go.id), https://orcid.org/0009-0000-6663-5648

1 National Research and Innovation Agency, Research Organization for Energy and Manufacture, Tangerang Selatan, Indonesia
2 Universitas Indonesia, Department of Mechanical Engineering, Depok, Indonesia
* Correspondence: kham001@brin.go.id

Abstract: This review synthesizes the current state of numerical simulation in friction stir welding (FSW) of dissimilar materials, with a particular focus on aluminum-polymer hybrid joints. The rapid expansion of this field, driven by the demand for lightweight, high-performance, and environmentally sustainable components in modern transportation sector, necessitates a rigorous understanding of the complex thermomechanical phenomena inherent to dissimilar systems. Therefore, the present study combines bibliometric mapping with a systematic analysis of Scopus-indexed literature from the past two decades. The analysis delineates the evolution of numerical modeling strategies, identifies key process parameters, and elucidates the thermomechanical fundamentals that govern joint performance. The present study employs an integrated approach, incorporating bibliometric insights, systematic reviews, and critical syntheses, to provide a comprehensive perspective on thermomechanical simulation in dissimilar FSW. The investigation highlights and analyzes the interplay between phase differences aluminum-polymer, thermomechanical behavior, and numerical convergence. The investigation further proposes optimization pathways that enhance accuracy and reliability while mitigating computational demands. This work provides a comprehensive reference for researchers and practitioners seeking to advance the predictive modeling and process optimization of aluminum-polymer FSW joints.

Keywords: numerical simulation, friction stir welding, dissimilar material, lightweight components

1 Introduction

The increasing demand for dissimilar material joining has grown in parallel with the development of lightweight structures across modern engineering sectors such as automotive, aerospace, and advanced manufacturing [1]. In transportation industries, multi-material combinations (metal-metal, metal-polymer, including aluminum and composites), enable significant weight reduction without compromising safety and performance, thereby contributing to improved fuel efficiency and reduced emissions [2]. Such dissimilar material joining enhances the strength-to-weight ratio and integrates distinct mechanical, thermal, and functional properties within a single component [3]. However, the application of conventional fusion welding methods to dissimilar materials faces fundamental limitations due to differences in melting points, thermal conductivity, thermal expansion coefficients, and metallurgical compatibility, which often lead to joint defects, thermal distortion, and reduced mechanical quality [4,5]. These challenges have driven the search for alternative joining technologies, and in this context, FSW offers significant advantages as a solid-state process, operating below the melting point of the materials, thereby minimizing metallurgical issues, reducing defect formation, and enabling the production of high-quality joints in various dissimilar material combinations that are difficult to weld using conventional techniques [6].

Despite the FSW offers significant advantages for joining dissimilar materials. However, the process still encounters complex technical challenges arising from differences in thermal, mechanical, physical, and metallurgical properties between the materials being joined. Variations in thermal conductivity and heat capacity lead to non-uniform temperature distributions, while mismatched mechanical properties, such as strength and ductility, result in distinct plastic deformation responses [5]. These responses often cause asymmetric material flow around the tool, particularly between the advancing and retreating sides. This generates thermal imbalance, which affects interfacial bonding quality. As a result, issues such as interfacial defects, non-homogeneous bonding, and high residual stresses emerge. Ultimately, these issues compromise the structural integrity and mechanical performance of dissimilar FSW joints [7,8].

In FSW, thermomechanical numerical simulation occupies a crucial role as a scientific approach to understanding and predicting the complex phenomena occurring during the welding process [9]. Through simulation, mechanisms of heat generation and distribution, material flow, plastic deformation responses of each material, and microstructural evolution at the interface can be analyzed in detail, which are often difficult to observe directly in experiments [10–12]. Furthermore, numerical simulation significantly reduces the reliance on experimental trial-and-error approaches that typically require high costs, long durations, and limited repeatability [13]. Simulation also enables systematic optimization of process parameters and tool design, thereby improving joint quality prior to experimental validation. Conversely, experimental studies are often constrained by measurement instrumentation, particularly under high-temperature and large-deformation conditions. As a result, a comprehensive understanding of thermomechanical interactions in dissimilar joints is unattainable without the support of advanced numerical simulation approaches [14–16].

This review article aims to provide a comprehensive and critical overview of the development of thermomechanical numerical simulations in FSW for dissimilar materials. The scope of the discussion focuses on thermomechanical aspects, including heat generation and distribution, material flow, and deformation and stress responses. In addition, experimental approaches are considered for more advanced dissimilar materials, particularly aluminum and polymers, which exhibit significant phase differences, as multi-material joining techniques are increasingly required in modern industries to produce lightweight yet strong joints. Systematically, the article is structured beginning with an introduction to the background and challenges of dissimilar FSW, followed by a discussion of fundamental thermomechanical phenomena, numerical modeling methods and techniques, a review of state-of-the-art research, and the identification of challenges and research gaps, before concluding with perspectives on future research directions.

2 Methodology

This study integrates two literature review methods: systematic literature review (SLR) and bibliometric analysis, using data from Scopus-indexed publications covering the last twenty years (2005–2025), with particular emphasis on research outcomes from the past decade. The search strategy employed the keywords: "(TITLE-ABS-KEY (fsw) AND TITLE-ABS-KEY (dissimilar) AND TITLE-ABS-KEY (numerical AND simulation))". Through a rigorous search and screening process, a total of 89 documents were identified, consisting of 66 journal articles, 16 conference papers, 4 review articles, and 3 conference reviews. The methodology applied in this study is systematically illustrated in **Figure 1** Methodology.

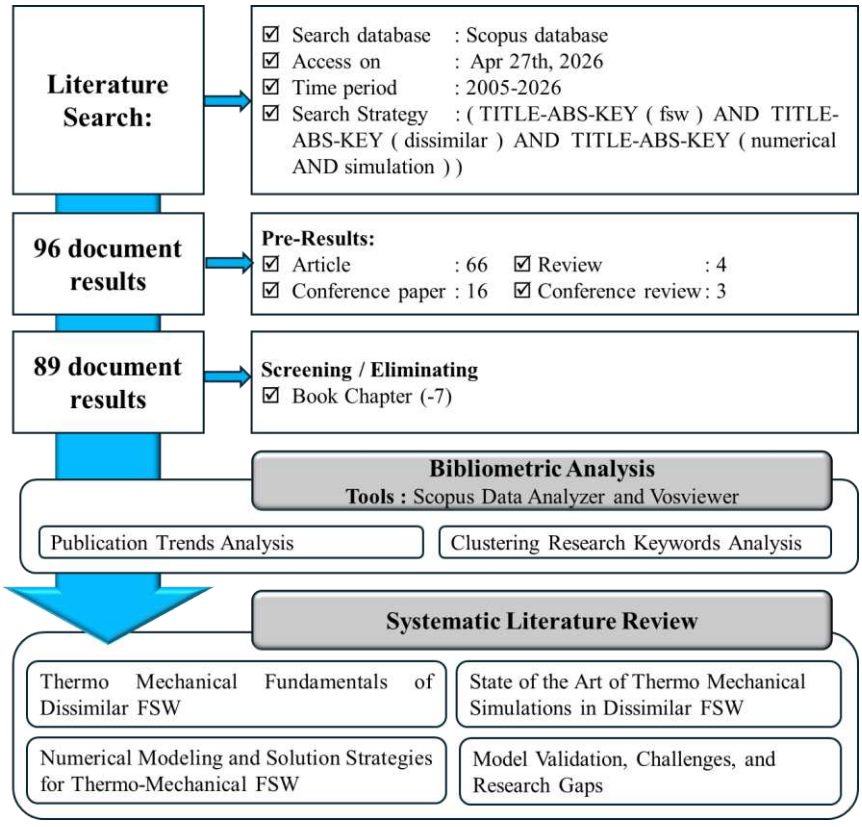


Figure 1 *Methodology*

Bibliometric analysis examines recent developments in the literature and proposes relevant future research directions. The results of this discussion highlight publication growth over the past two decades and a co-occurrence analysis that illustrates research clusters and trends within the field [17]. **Figure 2** presents the progression of publications, whereas **Figure 3** illustrates keyword clustering in studies conducted during the last twenty years.

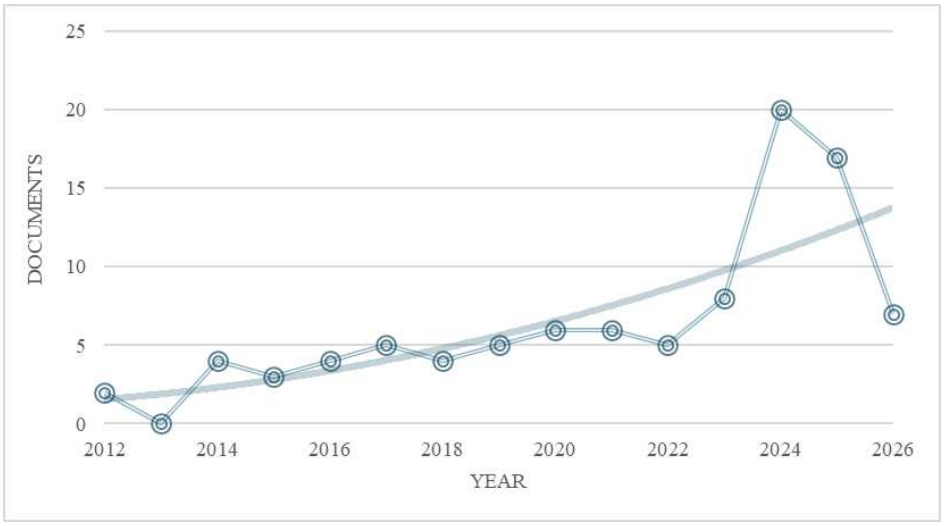


Figure 2 Publication Trends

As illustrated in **Figure 2**, the research was initiated in 2012 and remained relatively stable over the following decade. However, there has been a significant upsurge in publications in recent years, aligning with advancements in research and the increasing demand for computational numerical simulations in dissimilar material FSW. The annual output has averaged approximately five publications, peaking in the last three years with eight publications in 2023, twenty in 2024, and seventeen in 2025. As of April 2026, seven publications had already been recorded, and the trend continues to rise.

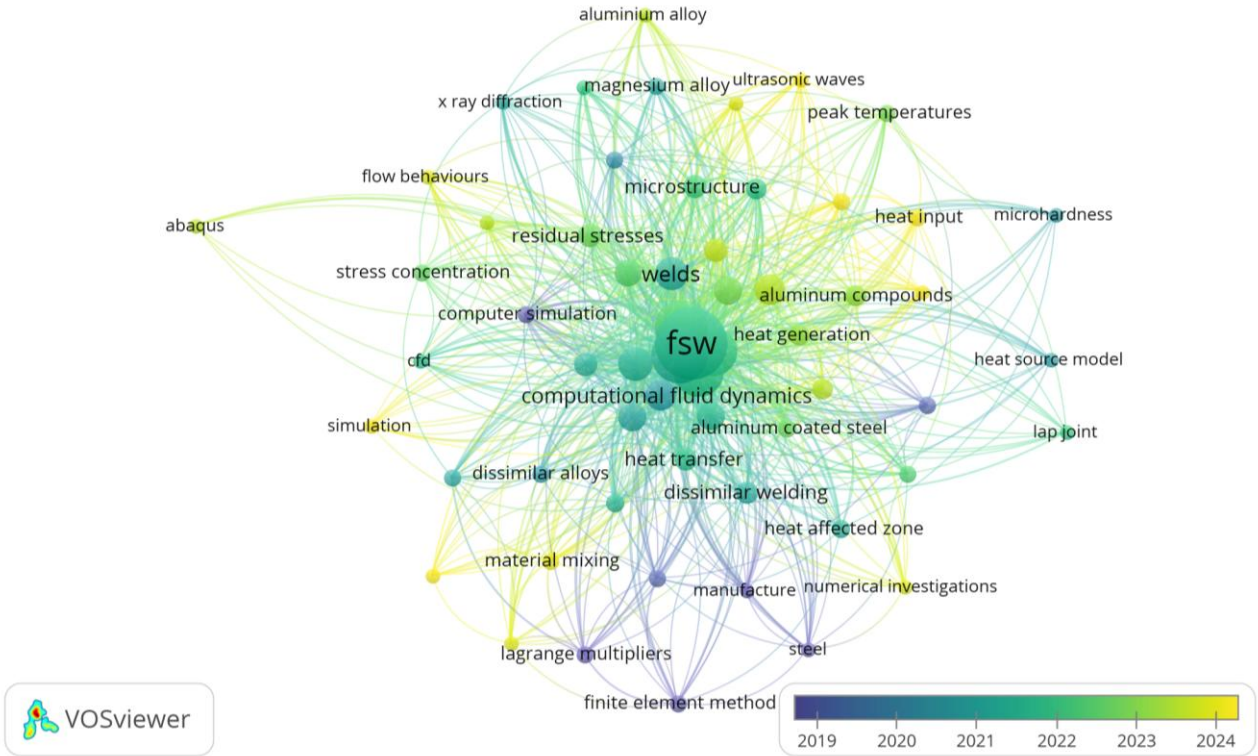


Figure 3 Co-occurrence Analysis

The co-occurrence analysis depicted in Figure 3 reveals that the numerical simulation research on dissimilar material FSW can be categorized into three primary domains: The first area of focus is thermal modeling and material flow, which is dominated by aluminum alloys (100), magnesium alloys (95), peak temperatures (80), flow behaviors (75), and heat input (60). The second area of focus is numerical methods, where Abaqus (65) and computer simulation (30) are more prominent compared to finite element method (1) or computational fluid dynamics (10). The third area of focus is emerging topics such as material mixing (1), dissimilar welding (1), and heat source modeling (15), which remain relatively rare. Research development has shifted from macro-level analysis (residual stresses 50) toward multi-physics modeling. However, the primary gap lies in experimental validation and the integration of microstructure (70) with welding parameters (45). Consequently, the most mature cluster pertains to the field of thermal modeling of aluminum–magnesium systems, while future research potential is concentrated in low-intensity but highly promising clusters such as material mixing for dissimilar joints using more integrated numerical approaches.

3. Thermomechanical Fundamentals of Dissimilar FSW

Fundamental thermomechanical aspects of FSW in dissimilar materials encompass complex integrated interactions involving heat generation, heat transfer, and material flow. These phenomena collectively govern the formation of interfacial bonding and asymmetric thermomechanical responses, thereby necessitating precise control of process parameters and the adoption of accurate numerical modeling approaches to achieve optimal joint performance. Numerical modeling of heat generation and material flow has been extensively investigated using various methods, with the most common approaches being the heat source model (HSM), computational solid mechanics (CSM), and computational fluid dynamics (CFD)[18].

3.1 Heat Generation and Heat Transfer Mechanisms

Heat generation in FSW is primarily governed by two dominant mechanisms: frictional heating arising from tool–material interaction and plastic deformation occurring within the stir zone [19]. Frictional heat is typically produced at the interface between the tool and the workpiece surface and often constitutes the major source of total heat input [19]. Up to 90% of the heat generation originates from the shoulder, while the pin contributes only minimally [20]. Nevertheless, within the stir zone, where intense material flow and high strain rates prevail, plastic deformation heat also provides a significant contribution and may even dominate depending on penetration depth, sliding conditions, tool geometry, and process parameters [19]. In dissimilar joints, differences in hardness and flow strength between the harder and softer materials lead to uneven heat distribution, resulting in asymmetric thermomechanical responses that influence the stability of material flow around the joint interface [21].

Beyond heat generation mechanisms, heat transfer in dissimilar FSW is strongly affected by differences in thermal properties, particularly thermal conductivity and specific heat capacity of the constituent materials [22]. Materials with high thermal conductivity tend to dissipate heat rapidly away from the weld zone, whereas those with low conductivity retain heat within the stirring region, thereby producing asymmetric temperature fields and complex thermal gradients [23]. These conditions are further influenced by process elements such as the tool shoulder, which plays a dominant role in generating frictional heat at the weld surface, and the backing plate, which governs heat dissipation through conduction at the underside of the joint. The interplay among material properties, tool design, and thermal boundary conditions determines the temperature distribution across the joint thickness and critically affects bond quality, plastic deformation, and the likelihood of defects in dissimilar FSW joints [22].

3.2 Material Flow and Plastic Deformation

Material flow and plastic deformation are governed by the complex interaction between the harder and softer materials surrounding the tool. The softer material tends to undergo plastic deformation earlier and flows more dominantly into the stir zone, whereas the harder material exhibits higher resistance to flow and only undergoes significant deformation under elevated temperature and strain rate conditions [24,25]. This imbalance in mechanical properties produces asymmetric flow patterns that directly affect mixing efficiency and stir zone stability [26]. The pin tool profile—such as threaded, flat, or eccentric designs—plays a crucial role in controlling material flow and mixing by enhancing vertical and horizontal migration, thereby improving local softening, reducing defects, and enhancing the mechanical properties of the joint [27].

Mixing and material flow in dissimilar FSW often generate complex flow patterns such as vortices, swirls, or laminar flow; however, under certain conditions, stagnation zones may also emerge near the joint interface [28]. These zones are characterized by restricted material movement and are frequently associated with defects such as joint line remnants or non-homogeneous interfacial bonding [29]. Furthermore, the placement of materials on the advancing side (AS) and retreating side (RS) plays a critical role in controlling flow patterns and plastic deformation distribution [25]. Positioning the harder material on the advancing side generally increases strain rate and local temperature, thereby promoting more effective

mixing, whereas suboptimal configurations exacerbate flow asymmetry and reduce the quality of dissimilar FSW joints [10,30]. Material flow and plastic deformation in dissimilar FSW are influenced by the complex interplay of parameters including tool design, process variables, material properties, and auxiliary techniques (e.g., ultrasonic assistance). Proper parameter optimization enhances mixing, refines grain structure, and suppresses defect formation.

3.3 Interfacial Mechanisms and Asymmetric thermomechanical response

The formation of interfacial bonding is primarily initiated by mechanical interlocking, which arises from the plastic flow of material during tool penetration and stirring, thereby producing mechanical anchoring around the interface [31,32]. This phenomenon occurs concurrently with asymmetric thermomechanical responses, triggered by differences in heat generation between the advancing side (AS) and retreating side (RS) due to the combined effects of tool rotation and traverse motion. Consequently, unbalanced deformation and strain rate conditions are established. The AS generally experiences higher plastic deformation and greater heat generation, which subsequently produces non-symmetric temperature distributions both laterally and across the joint thickness [33]. Such non-uniform thermal fields directly influence material flow, microstructural evolution, and residual stress formation. Therefore, controlling thermomechanical conditions is crucial to balance the contributions of mechanical interlocking, diffusion bonding, and intermetallic compound (IMC) formation, underscoring the importance of accurate coupled numerical modeling in the analysis and optimization of dissimilar FSW joints [34].

4. Numerical Modeling and Solution Strategies for Thermomechanical FSW

4.1 Thermomechanical Modeling Fundamentals

Numerical modeling has emerged as a highly significant approach for understanding and optimizing thermomechanical phenomena in FSW, given that the process involves complex interactions among heat generation, material flow, and microstructural evolution [35]. An accurate numerical modeling framework is essential to reliably predict temperature distribution, residual stress formation, and joint quality, thereby reducing reliance on costly experimental approaches and accelerating process development.

Table 1 Thermomechanical Modeling Fundamentals: Aspects, Insights, and Gaps

Aspect	State-of-the-Art Insights	Limitations / Gaps	References
Governing Equations	Fully coupled thermomechanical models (mass, momentum, energy) using ALE, adaptive meshing, and temperature-dependent properties	High computational cost; limited high strain rate data; validation challenges	[35–38]
Constitutive Models (Dissimilar Materials)	Norton-Hoff, Sheppard-Wright, CDRX, DDRX, viscoplastic models; microstructural evolution included in advanced models	Insufficient high strain rate/temperature data; calibration complexity; asymmetric microstructure	[39,40]
Friction/Contact/Boundary Modeling	Advanced friction laws (Norton, Tresca, enhanced models), partial sticking/slipping, adaptive meshing, ALE for contact	Empirical calibration; incomplete temperature/strain rate dependence; interface complexity	[41–43]
Assumptions & Simplifications	Simplified heat generation, empirical friction, semi-coupled models for efficiency	Reduced accuracy in residual stress/microstructure, especially in complex/dissimilar joints	[44,45]
AI/ML Integration	Real-time optimization, parameter tuning, defect prediction, digital twins	Data scarcity; limited real-time industrial deployment	[46–48]

Fundamental modeling of FSW is based on the conservation equations of mass, momentum, and energy, which are solved in a coupled manner to represent material flow, mechanical response, and thermal evolution during the process. The momentum equation is employed to capture mechanical behavior through solid mechanics or fluid flow formulations, while the energy equation models heat transfer by incorporating frictional heating and plastic deformation dissipation as the primary energy sources [37]. These equations are typically implemented using finite element method (FEM) and CFD with Lagrangian, Eulerian, or Arbitrary Lagrangian–Eulerian (ALE) formulations to accommodate large deformations and

evolving interfaces [49,50]. The accuracy of simulations strongly depends on the integration of temperature- and strain-rate-dependent material properties, which remains challenging due to limited experimental data under extreme stir zone conditions. The selection of constitutive models and interface modeling plays a crucial role in realistically representing material behavior under high-temperature and high strain-rate conditions [42]. Literature indicates that metallic materials are generally modeled using viscoplastic approaches, such as the Norton–Hoff or Sheppard–Wright models, which effectively capture plastic flow responses in the stir zone, whereas non-metallic or hybrid systems are represented using nonlinear models tailored to viscoelastic or viscoplastic characteristics [51]. Heat generation is quantitatively modeled through modified frictional phenomena and heat distribution, with tool rotational speed identified as the dominant parameter. Significant progress has been achieved through advances in computational techniques and the integration of artificial intelligence and machine learning (AI/ML) for real-time parameter optimization [46,52]. Nevertheless, limitations in material property data under high-temperature and extreme strain-rate conditions, along with challenges in consistent calibration at dissimilar material interfaces, remain key research gaps. Therefore, future developments should focus on more comprehensive experimental validation, strengthening coupled physical models, and applying hybrid numerical strategies to enhance predictive accuracy and computational efficiency in thermomechanical FSW simulations.

4.2 Numerical Formulations and Solution Techniques

Dissimilar FSW involves complex and interrelated thermomechanical phenomena such as heat generation, plastic deformation, and dynamic material flow, which pose significant challenges in both experimental investigations and numerical simulations. This review provides insights into recent advances in technical solution strategies for numerical simulation of FSW, with emphasis on FEM, ALE and Coupled Eulerian–Lagrangian (CEL) approaches, CFD-based models, and hybrid modeling frameworks, as well as a comparative analysis of the advantages of integrated versus sequential thermomechanical simulations.

Table 2 Numerical Techniques: Strengths, Limitations, Relevance

Numerical Technique	Strengths	Limitations	Relevance	References
Lagrangian FEM	Accurate thermomechanical analysis; established frameworks	Mesh distortion under large deformations; less effective for material flow	Preferred for stress/strain and temperature analysis	[49]
Eulerian FEM	Handles large deformations; effective for material flow	Difficulty with tool advancement; less suited for stress analysis; Poor boundary resolution	Used for fluid-like material flow modeling	[49]
ALE (Arbitrary Lagrangian-Eulerian)	Combines Lagrangian/Eulerian strengths; adaptive meshing; robust for large deformations	Requires remeshing; complex interface treatment; Higher computational cost	Good for heat-affected zone and complex tool geometries	[53]
CEL (Coupled Eulerian-Lagrangian)	Captures volumetric defects; robust for large deformations; accurate material mixing	High computational cost	Best for defect prediction and dissimilar material FSW	[53–55]
Meshless Methods (NEM, SPH)	No mesh distortion; accurate for large deformations and interface tracking	High computational cost; less mature for industrial use	Promising for complex flows and microstructure evolution	[34,56,57]
CFD-based Modeling	Effective for material flow, temperature, and non-Newtonian viscosity	Less suited for stress/strain; boundary condition sensitivity	Used for tool geometry optimization and flow visualization	[58,59]
Hybrid CFD-FEM	Integrates strengths of CFD and FEM; multi-physics, multi-scale modeling	Increased model complexity; computationally intensive	Enables fully coupled simulations and advanced process control	[50,59]

Coupled Thermo-mechanical	High accuracy for residual stress, process asymmetry, and feedback effects	High computational cost	Essential for local phenomena and defect prediction	[36,60,61]
Sequential Thermomechanical	Computationally efficient; suitable for global stress prediction	May neglect feedback effects; less accurate for local phenomena	Used for large-scale or post-process analyses	[36,60,61]

Material flow modeling in FSW has generally been developed using FEM with Lagrangian and Eulerian formulations. The Lagrangian formulation follows material movement, making it effective in capturing stress, strain, and temperature fields in detail, though it tends to suffer from mesh distortion under large plastic deformation in the stir zone [49]. Conversely, the Eulerian formulation maintains a fixed mesh in space and allows material to flow through it, offering greater stability for modeling intensive material flow, albeit with limitations in representing moving boundary conditions and local mechanical responses [54]. To accommodate large deformations and complex material flow, ALE and CEL approaches have become increasingly prevalent in modern FSW simulations. ALE enables adaptive mesh movement independently of material flow, thereby reducing mesh distortion while maintaining thermomechanical accuracy [62]. CEL combines the strengths of Eulerian and Lagrangian formulations by modeling the tool as a Lagrangian domain and the workpiece as an Eulerian domain, proving highly effective in predicting material mixing and interfacial phenomena in dissimilar joints [54,55,63].

In the context of dissimilar FSW, the choice of numerical formulation must consider trade-offs between accuracy and computational efficiency. The Lagrangian formulation excels in detailed local analysis but is constrained by mesh distortion, whereas the Eulerian formulation offers stability for material flow but lacks precision in stress and deformation evaluation. ALE provides a balance between stability and accuracy, while CEL delivers the most realistic representation of material flow and volumetric defects, though at higher computational cost. Literature emphasizes that no single approach is universally superior, and the choice of method depends strongly on the simulation objectives and the complexity of the material system under analysis [52,63].

Numerical techniques and solution strategies in FSW simulations highlight that the success of numerical modeling is determined by the selection of methods capable of balancing physical accuracy and computational efficiency. Literature confirms that FEM with Lagrangian formulation is advantageous for detailed thermomechanical analysis, particularly in predicting temperature and stress, but faces limitations due to mesh distortion under large plastic deformation, which are addressed through Eulerian, ALE, and CEL formulations. CFD-based approaches and hybrid CFD–FEM models are increasingly adopted for their ability to realistically represent plasticized material flow and heat generation, especially in dissimilar joints with complex flow patterns. Meanwhile, the choice between fully coupled thermomechanical simulations and sequential simulations reflects a fundamental trade-off between predictive accuracy of feedback phenomena and computational efficiency.

4.4 Advanced and Multi-Physics Simulation Approaches

Advanced approaches in FSW simulations employ CFD and particle-based methods to model the behavior of highly plasticized material in the stir zone. Within the CFD framework, the material is often treated as a non-Newtonian fluid whose viscosity depends on temperature and strain rate, thereby enabling detailed predictions of material flow and heat distribution. Particle or meshless methods provide additional advantages in handling extreme deformations and interface tracking, although their application remains limited due to high computational demands and complex mechanical integration [50,58].

As accuracy requirements increase, FSW simulations have evolved from sequential approaches toward fully coupled thermomechanical models, in which thermal and mechanical fields are solved simultaneously. Fully coupled models capture feedback mechanisms between heat generation, plastic deformation, and material property evolution, thus offering more realistic predictions of temperature, material flow, and residual stress. However, this approach incurs high computational costs, making sequential or semi-coupled models still widely used for global analyses as a compromise between accuracy and efficiency [36,60].

Beyond thermal–mechanical coupling, recent developments also emphasize multi-physics integration that combines thermomechanical simulations with metallurgical models. This integration enables the modeling of microstructural evolution, interfacial phase formation, and defect initiation under extreme welding conditions. Literature indicates that although complex and requiring careful calibration, multi-physics approaches provide the most comprehensive framework for linking process parameters with final joint quality, particularly in dissimilar FSW where physical and thermochemical interactions

are highly complex. Nonetheless, challenges remain regarding computational cost and the availability of material data [46,48].

5. State-of-the-Art of Thermomechanical Simulations in Dissimilar FSW

5.1 Aluminum-Based Dissimilar Joints

Recent studies on aluminum-based dissimilar joints, including Al–Al, Al–Mg, and Al–Steel/Ti, have highlighted the importance of thermomechanical simulations in predicting joint performance [46]. Finite element (FE) and CFD models have demonstrated that differences in thermal conductivity and flow stress between dissimilar alloys lead to asymmetric temperature fields and heterogeneous material flow. For instance, simulations of Al–Mg joints revealed that the magnesium side experiences higher localized temperatures due to its lower thermal conductivity, which directly influences residual stress distribution and joint strength[64]. Sarfaraz et al. (2025) investigated friction stir welding of dissimilar aluminum alloys AA2024-T3 and AA5086-O using a sequentially coupled thermomechanical 3D FEM model, and the results demonstrated that tool rotational speed exerted a more dominant influence than traverse speed on temperature distribution and residual stress, with longitudinal stress exceeding lateral stress and the maximum residual stress being higher on the retreating side (AA5086-O) compared to the advancing side (AA2024-T3). The simulation results indicate that longitudinal residual stress is more dominant than lateral stress, and the longitudinal residual stress for all welding configurations after cooling to room temperature [65].

5.2 Metal–Nonmetal Dissimilar FSW

The joining of metals with nonmetals, such as Al–Polymer and Al–Composite, presents unique challenges due to the extreme differences in thermal and mechanical properties. Nevertheless, the inherent variations in the chemical, physical and thermal properties of the base materials introduce significant challenges in the joining process, thereby requiring the development of new manufacturing technologies [52]. Hosny (2024) reported that the interfacial temperature distribution in friction stir welding of AA5052 aluminum alloy to polypropylene (PP) is difficult to obtain experimentally, leading to the use of numerical thermal simulation, where process temperatures were monitored with infrared cameras and thermocouples validated numerical modeling determined the cross-sectional temperature distribution [66]. The capability of infrared cameras and thermocouples measurements is constrained to the surface area and the area extending beyond the shoulder. Meanwhile, the interface area between the plates and the area under the shoulder can be captured using thermal distribution modeling based on numerical simulation, as shown in Figure 4.

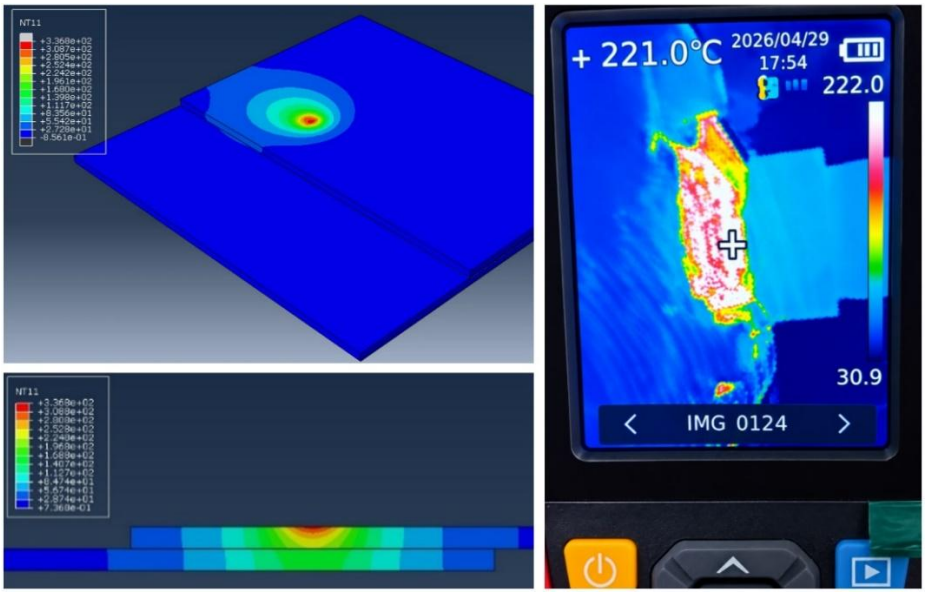


Figure 4 *Temperature distribution modeling at AA6061- Polycarbonate Joint*

5.3 Prediction of Key Process Outputs

Modern thermomechanical simulations have become increasingly capable of predicting critical process outputs such as temperature distribution, material flow patterns, forces and torque, and residual stress. Coupled FE–CFD models have successfully replicated the dynamic evolution of temperature fields and flow vortices around the tool pin, providing insights into defect formation mechanisms. Predictive frameworks for thermomechanical simulations in FSW are computational

tools used to model heat generation, severe plastic deformation, and material flow without extensive experimental trials [66]. Yousef (2026) developed and validated a comprehensive digital twin framework for FSW by integrating multi-physics finite element simulations, real-time sensor synchronization, and machine-learning-based predictive analytics, and the findings demonstrated that the model reliably predicted temperature distribution, material flow, and residual stress evolution, while experimental validation confirmed high predictive accuracy for mechanical properties and defect detection[67]. The integration of digital twin technology with machine learning has significantly enhanced its predictive and analytical capabilities. [66].

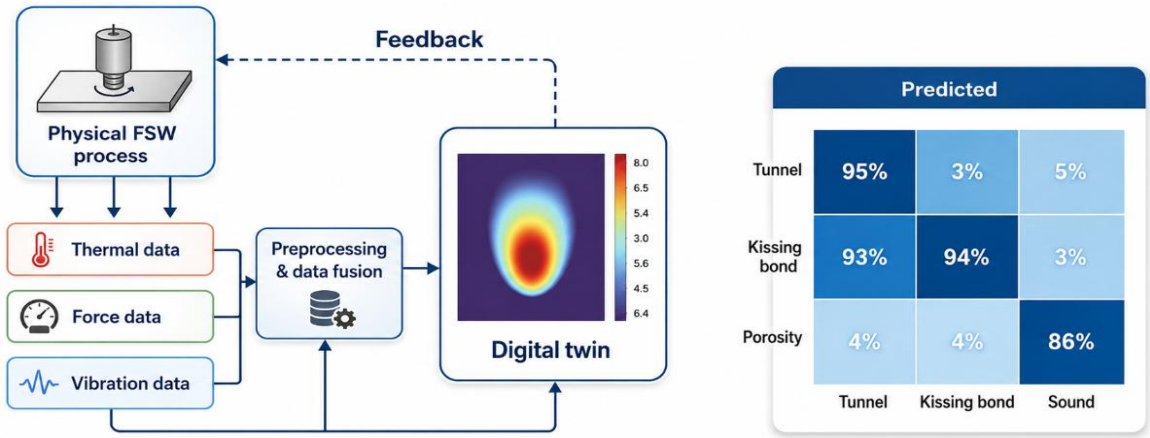


Figure 5 Comparing predicted and Experimental FSW

5.4 Comparison of Modeling Strategies

The comparison of modeling strategies reveals a trade-off between accuracy and computational cost. Simplified models, such as two-dimensional FE approaches, offer reduced computational demand but often fail to capture three-dimensional flow complexities. Conversely, fully coupled thermomechanical models with adaptive meshing provide high fidelity predictions at the expense of significant computational resources. Hybrid strategies, combining Eulerian, Lagrangian, and ALE formulations, have emerged as promising solutions, balancing accuracy and efficiency. Comparison of the advantages of numerical methods in FSW simulations on different materials is shown in Table 3.

Table 3 *Comparative Strengths of Numerical Methods in Dissimilar FSW Simulation*

Method	Heat Prediction	Material Flow	Residual Stress	Defect Prediction	Microstructure	Computational Cost
FEA (ALE/CEL)	High	High	High	High	Moderate	High
CFD (VOF)	High	High	Low	Moderate	Low	Moderate
TPM	Moderate	Moderate	Moderate	Low	Low	Low
Multiphysics	High	High	High	High	High	Very High

6. Numerical Investigation for Aluminum Polymer Joint

6.1 Structural Model

To map how heat spreads across the joint area during the friction stir lap welding (FSLW) process between Al6061 and polycarbonate (PC), we developed a three-dimensional transient thermal simulation model using Abaqus Standard software. In the FSLW process, heat is generated from two main sources: surface friction caused by the tool shoulder, and friction and plastic deformation caused by the pin penetrating the top aluminum plate. This generated heat then propagates into the polycarbonate plate beneath it via conduction. The transient heat flow within these two materials is governed by the following 3D heat conduction equation:

$$\frac{\partial}{\partial x}\left(k\frac{\partial T}{\partial x}\right)+\frac{\partial}{\partial y}\left(k\frac{\partial T}{\partial y}\right)+\frac{\partial}{\partial z}\left(k\frac{\partial T}{\partial z}\right)=\rho C_p\frac{\partial T}{\partial t}$$

Where, k is the thermal conductivity, whose value varies with temperature; ρ is the density of the material; C_p represents the specific heat capacity; and t is the welding duration.

The geometric model in this simulation was created to reflect laboratory conditions, in which an AA6061 top plate (3 mm thick) is stacked on top of a PC plate (3 mm thick) with an overlap width of 50 mm, detail in Figure 6. This model was divided into small elements using hexagonal 8-node linear heat transfer bricks (DC3D8). The element size in the critical areas (primarily around the pin penetration path and the interface between the two materials) was refined to $1 \times 1 \times 1$ mm^{3}to capture the sharp temperature gradients, while areas farther from the weld line used a coarser mesh size ($2 \times 1 \times 1$ mm^3). This mesh configuration results in 46,781 nodes and 36,921 elements.

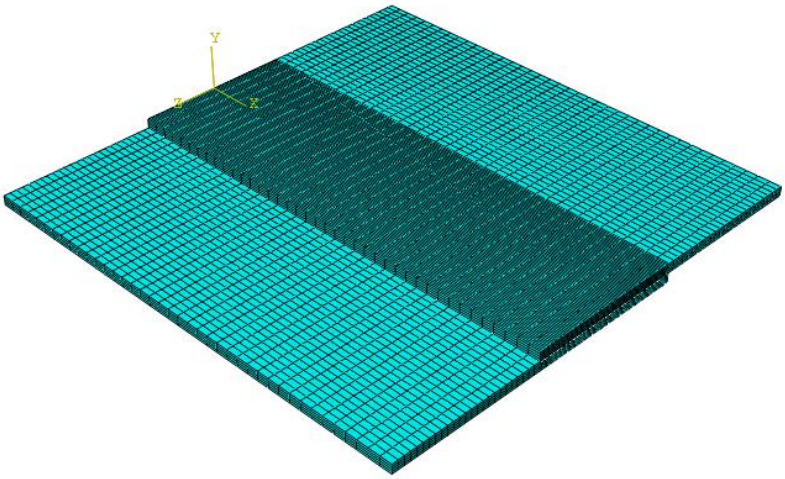


Figure 6. Numerical model mesh

6.2 Boundary Conditions and Heat Source Movement

The boundary conditions in this model are designed to simulate heat loss to the free atmosphere and to the base. The top and bottom surfaces of the plate in contact with the outside air are assigned convective cooling values using the following equations:

$$-k(T)\frac{\partial T}{\partial z} = h(T - T_{\infty})$$

Where h is the convective heat transfer coefficient, and T_{∞} } is the ambient temperature, which is 25°C. Meanwhile, the side edges of the plate are assumed to be insulated to simplify the calculations.

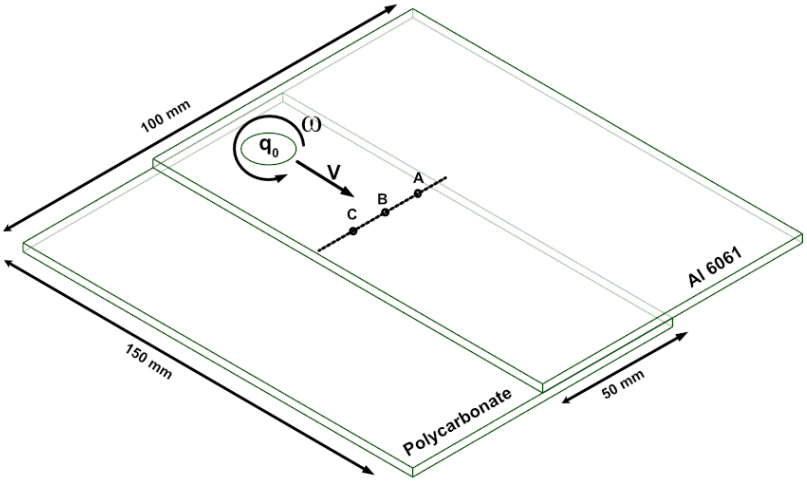


Figure 7. Boundary condition of numerical simulation

The heat energy from the tool is modeled as a moving heat source consisting of two main components: the surface heat flux from the shoulder and the volumetric/surface heat flux from the pin. The distribution of these heat fluxes is integrated into the simulation using the user-defined subroutine DFLUX. Heat from the shoulder is assumed to increase linearly from the outer boundary of the pin to the outer edge of the shoulder diameter (r). Meanwhile, heat from the pin is distributed along the depth of the pin's penetration into the AA6061 plate (set such that the tip of the pin provides an optimal thermal pressure effect near the polymer interface without damaging the PC plate beneath it).

Modeling the heat source in the FSLW process using the DFLUX subroutine represents the distribution of the moving heat flux on the workpiece surface. The tool angular velocity (Ω) is converted from rotational speed (ω) using the equation:

$$\Omega = \omega \times \frac{2\pi}{60}$$

Where Ω is the angular velocity (rad/s) and ω is the rotational tool speed (rev/min). The total heat power (Q) yan generated by friction between the tool shoulder and the workpiece is calculated based on a friction model, expressed by the equation:

$$Q = \eta \cdot \frac{2}{3} \cdot \pi \cdot \mu \cdot P_{\text{ax}} \cdot \Omega \cdot R_0^3$$

Where Q is the total heat power (W), η is the efficiency of heat transfer to the workpiece, μ is the coefficient of friction, P_{ax} is the axial pressure (Pa), and R_0 is the radius of the shoulder (m). The position of the heat source center along the X-axis (X_C) is time-dependent to represent the tool's movement along the weld path, defined as:

$$X_C(t) = \{X_0 \quad \text{if } t < t_{\text{start}}\ X_0 + V \cdot (t - t_{\text{start}}) \quad \text{if } t \geq t_{\text{start}}$$

where X_0 is the initial position of the tool on the X-axis (m), V is the tool's velocity (m/s), t is the simulation time (s), and t_{start} is the start time of the tool's movement (s). The position of the center of the heat source along the Z-axis is kept constant such that $Z_C = Z_0$, where Z_0 is the initial position of the device along the Z-axis (m). The square of the distance from the material point to the center of the heat source (d^2) is calculated using the equation:

$$d^2 = (X - X_C)^2 + (Z - Z_C)^2$$

where X and Z are the coordinates of a material point on the surface of the workpiece (m). The spatial distribution of heat flux on the surface of the workpiece is modeled using a 2D Gaussian distribution, which is expressed as:

$$q_0(X, Z, t) = \frac{3Q}{\pi R_0^2} \exp\left(-\frac{3d^2}{R_0^2}\right)$$

Where q_0 is the heat flux intensity (W/m²). The application of the heat flux is limited to the area within the radius of the device's shoulder, which is mathematically represented using the Heaviside function (H). Overall, the surface heat flux applied to the model (q) is expressed as:

$$q(\mathbf{r}, t) = \frac{3Q}{\pi R_0^2} \exp\left(-\frac{3|\mathbf{r} - \mathbf{r}_C(t)|^2}{R_0^2}\right) \cdot H(R_0 - |\mathbf{r} - \mathbf{r}_C(t)|)$$

where $r = (X,\ Z)$is the position vector of the material point, $r_C(t) = (X_C,\ Z_C)$is the position vector of the heat source center, and H is the Heaviside function, which takes the value 1 if the argument is greater than 0, and 0 if the argument is less than or equal to 0.

All the FSW process parameters used in this simulation are presented in Table 4.

Table 4. Process parameter for numerical simulation

Parameter	Symbol	Value	Unit
Rotation speed	RPM	1660	rev/min
Welding speed	V	0.0008	m/s
shoulder radius	R_0	0.0075	m
Axial Pressure	P_{ax}	4.25×10^6	Pa
Coefficient of friction	μ	0.30	-
Thermal Efficiency	η	0.90	-
Initial Position of the X-Axis	X_0	0.020	m
Initial Position of the Z-Axis	Z_0	0.0	m
Start Time of Movement	t_{start}	10.0	s

6.3 Interface Conductance and Thermal Properties of Materials

The aluminum plate is textured and is subjected to direct pressure and friction from the pin penetration, the thermal resistance at the interface between AA6061 and PC will change dynamically. To ensure that heat transfer in this simulation closely approximates reality, we incorporated the GAPCON user subroutine to set the interface gap conductance (K). This interface area is divided into three dynamic zones that move in accordance with the tool's position:

- K_1: The zone already traversed by the pin and shoulder (the area that has already been joined).
- K_2: The zone directly under the influence of the tool (shoulder and pin penetration) that experiences the highest thermomechanical stress.
- K_3: The zone in front of the tool that has not yet been affected by the welding process.

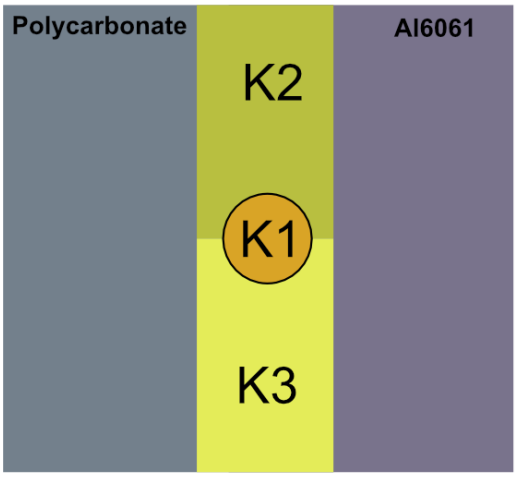


Figure 8. Subroutine GAPCON application in FSLW

The values of the heat flux amplitude (q_o) and the gap conductance coefficients ($K_1 and K_2$) are determined iteratively using the Inverse Heat Conduction Method (IHCM). This is done by minimizing the error (f) between the simulated temperature results (T_i^s) and the actual data from thermocouple readings (T_i^{exp}):

$$f = \sum_{i=1}^{n} \left(T_i^s - T_i^{exp}\right)^2$$

This simulation also incorporates the temperature-dependent nonlinear thermophysical properties of both materials. For AA6061, the thermal conductivity ranges from 160 to 220 W/m˚C, with a specific heat of 900 to 1150 J/kg˚C. Meanwhile, for amorphous polycarbonate (PC), the important thermal transition around its glass transition temperature ($T_g \approx 145°C$) is included in detail so that the simulation can capture the moment when this polymer begins to soften due to heat transfer from the top plate.

6.4 Results and Discussion: Numerical Thermal Analysis

Simulations at nodes A, B, and C show the results presented in Figure 9. At the 80th second, the temperatures on the Al surface are 191.03, 248.32, and 182.67 in Celsius. The temperature at node B is the highest because it is located at the center of the tool, while the temperature difference between nodes A and C can be explained based on their relative positions with respect to the tool's direction of motion and the Gaussian heat distribution gradient applied to the model. Node A, which has a higher temperature than Node C, indicates that this location is closer to the effective heat source path or is on the side where heat accumulation is greater. In the FSLW process, this phenomenon is generally related to the difference between the advancing side (AS) and the retreating side (RS). On the advancing side, the direction of tool rotation is in the same direction as the translational motion, so the relative velocity between the tool and the material is higher, resulting in greater plastic deformation and heat generation compared to the retreating side.

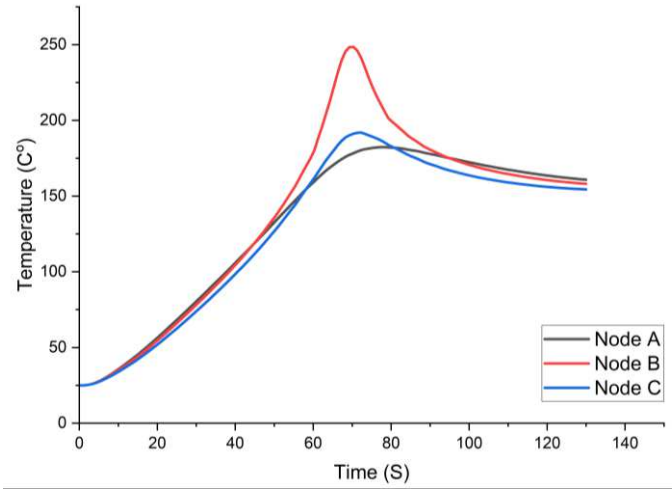


Figure 9. Temperature history at nodes A, B, and C on the Al surface

Observing the temperature mapping results during the welding process, when it is running stably, the heat field in the joint area exhibits unique characteristics due to tool penetration. Figure 10 shows a visualization of a cross-section of the joint perpendicular to the welding direction.

The highest temperature in the entire assembly is always concentrated within the Al6061 metal plate, precisely at the wall of the area in direct contact with the pin and beneath the shoulder's grip. Due to the high thermal conductivity of Al6061, this heat spreads rapidly laterally across the aluminum plate.

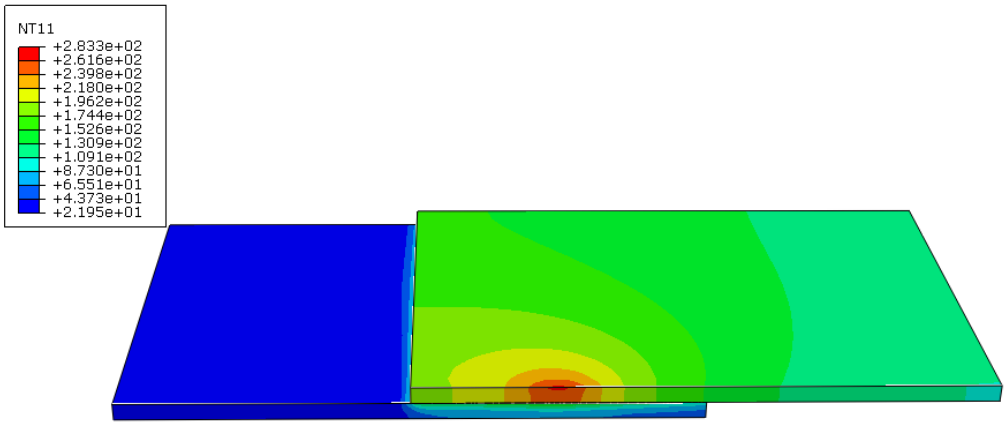


Figure 10. Cross-section showing the temperature distribution during welding.

However, a very sharp vertical temperature gradient occurs in the polycarbonate plate beneath it. The high temperature is confined and penetrates only the top layer of the polycarbonate that is in direct contact with the aluminum interface. The lower polycarbonate layer remains safely close to room temperature. This localized heat demonstrates that the combination of pin length and welding parameters used successfully channels thermal energy effectively to soften the polymer contact surface, without causing widespread melting or structural failure of the entire polycarbonate plate body.

This "heat trapping" pattern is in close alignment with the findings of Sheikh-Ahmad et al. on AA5052-CF/PEEK joints and Hosny et al. on AA5052-PP joints[66,68]. Because polymers have a much lower thermal conductivity than aluminum, heat transferred from the top plate cannot immediately propagate downward but instead accumulates on the upper surface of the polycarbonate. Our modeling of the dynamic gap conductance values (K_1, K_2, K_3) using the GAPCON subroutine successfully captured this behavior accurately. The sharp spike in the K_2 conductance value directly beneath the tool reflects the tightness of the thermomechanical contact caused by the tool's axial pressure, as well as the moment when the softened polycarbonate begins to be forced into the textured voids on the aluminum surface.

The temperature history at this interface ultimately becomes the key factor determining the strength of the mechanical interlocking that forms. The peak interface temperature of $248,32°C$ that we obtained is more than sufficient to exceed the glass transition temperature of polycarbonate ($T_g \approx 145°C$), allowing the polymer to soften and flow smoothly to interlock with the burrs/hooks created by the aluminum texture. However, maintaining the temperature within a safe "process window" is absolutely crucial. As explained by Hosny et al. in their polymer thermal analysis, if the applied heat input is excessive and exceeds the polymer's thermal resistance threshold, the polymer will degrade and release gas. This trapped gas then forms bubbles or micro voids as it solidifies, which later become weak points and lead to joint failure. Thus, the FSLW parameters and heat control in this simulation were found to be within the optimal range: hot enough to soften the polymer surface for a strong mechanical interlock, but not so hot as to damage the polycarbonate structure itself.

7. Future Perspectives and Conclusions

7.1 Future Perspectives

- Constitutive Model Development: future work should generate high strain rate and temperature data for dissimilar materials to establish standardized, validated constitutive laws.
- Friction and Heat Generation Models: research must prioritize the creation of unified, experimentally validated friction models that capture temperature- and rate-dependent dissipation across tool regions.
- Hybrid and Multi-Scale Numerical Frameworks: adaptive simulation strategies that dynamically switch between Eulerian and Lagrangian regimes, while bridging microstructural evolution with macroscopic parameters, represents a critical frontier.
- AI/ML and Digital Twin Integration: expanding physics-informed machine learning and digital twin technologies will enable real-time process optimization, predictive maintenance, and intelligent adaptive control.

- Advanced Experimental Validation: large-scale, multi-modal campaigns and real-time in-situ measurements of temperature, strain, stress and microstructural evolution are essential to calibrate and refine numerical models.
- Expanded Material Systems and Assisted Techniques: exploration of novel dissimilar material combinations and assisted FSW methods for long-term joint performance, lightweight material, and corrosion studies will broaden application domains.

7.2 Conclusions

- The accurate thermomechanical modeling of dissimilar FSW requires temperature-dependent, coupled numerical formulations to capture frictional and plastic heat generation, as property mismatches drive asymmetric heat flow and steep gradients; recognizing and mitigating these asymmetries through integrated modeling and experimental validation is essential for optimizing joint performance.
- Advances in coupled FEM, ALE, and CEL approaches have enabled robust predictions of thermo-mechanical fields and residual stresses, while adaptive meshing and temperature-dependent friction models enhance accuracy; yet persistent challenges in IMC formation, microstructural evolution, computational cost, and unified frictional heat modeling underscore the need for high-fidelity, multi-scale simulations that integrate emerging multi-physics, predictive analytics AI-driven approaches, and supported by comprehensive experimental validation.
- Thermomechanical modeling of FSLW aluminum polymer joints provide reliable insights into heat transfer, temperature distribution, and interfacial behavior, revealing localized hotspots around the pin and confined heating in the polymer layer that enable plasticity and mechanical interlocking without structural degradation. Therefore, maintaining interface temperatures within a safe process, supported by controlled simulations and experimental validation, is thus essential for optimizing process temperature to enhance joint strength and preventing polymer damage.

Acknowledgements

This study was supported by the National Research and Innovation Agency (BRIN) of Indonesia for providing the scholarship (No.93/II.5/HK/2025) and research grant (No. 6/III.3/HK/2026). The authors gratefully acknowledge the invaluable guidance and continuous support of Prof. Cuk Supriyadi, Prof. Ario Sunar Baskoro, Prof. Gandjar Kiswanto and Dr. Muizuddin Azka for their significant advisory for this study.

Author Contributions

Khamda Herbandono: Conceptualization, Methodology, Investigation, Data Curation, Writing – Original Draft Preparation, Formal Analysis. **Harry Purnama:** Conceptualization, Visualization, Writing – Review & Editing, Formal Analysis. **Dede Santoso:** Conceptualization, Writing – Review & Editing, Formal Analysis. **Katri Yulianto:** Writing – Review & Editing, Formal Analysis.

Declaration of generative AI and AI-assisted technologies in the writing process

During the preparation of this manuscript, the authors used Vosviewer to visualize the mapping of research keywords (bibliometric), Microsoft Copilot and TrinkaAI to enhance grammar, improve language clarity, and refine readability. Following the use of these tools, the authors carefully reviewed and edited the content as necessary and accept full responsibility for the accuracy, integrity, and originality of the final manuscript.

Conflict of interest

The authors declare that they have no known competing financial interests or personal relationships that could have appeared to influence the work reported in this paper.

References

[1] Y.Y. Jang, J.C. Ha, D. Lee, Y. Lee, S.Y. Nam, S.B. Yang, D.J. Kwon, Dissimilar material bonding technology for lightweight future mobility: A review, Polym. Test. 129 (2023). https://doi.org/10.1016/j.polymertesting.2023.108281.

[2] S.A. Choudry, J. Kaspar, M. Vielhaber, D. Landgrebe, Concurrent assessment of material and joining technology in lightweight engineering, 2019. https://doi.org/10.1007/978-3-030-04290-5_15.

[3] S. Siengchin, A review on lightweight materials for defence applications: Present and future developments, Def. Technol. 24 (2023) 1–17. https://doi.org/10.1016/j.dt.2023.02.025.

[4] S. Sasabe, T. Iwase, T. Matsumoto, Y. Hattori, T. Miono, Dissimilar metal joining of aluminum alloys to steel in MIG braze welding by using the advanced hot-dip aluminized steel sheet, Yosetsu Gakkai Ronbunshu Q. J. Jpn. Weld. Soc. 27 (2009). https://doi.org/10.2207/qjjws.27.55s.
[5] Tanmay, Z. Alam, S.S. Panda, A Review on Joining of Dissimilar Metals with Highly Differential Thermomechanical Properties, J. Mater. Eng. Perform. 34 (2025) 8219–8231. https://doi.org/10.1007/s11665-024-10279-y.
[6] M.M. Patel, V.J. Badheka, A review on friction stir welding (FSW) process for dissimilar aluminium to steel metal systems, Weld. Int. 38 (2024) 91–115. https://doi.org/10.1080/09507116.2023.2291064.
[7] V. Chitturi, S. Rao Pedapati, M. Awang, A Review on Process Parameters and their effects on Dissimilar Friction Stir Welding of Aluminium and Steel Alloys, in: Iop Conf. Ser. Mater. Sci. Eng., 2019. https://doi.org/10.1088/1757-899X/551/1/012003.
[8] S. Ganguly, Welding of dissimilar metals, 2023. https://doi.org/10.1016/B978-0-323-90552-7.00014-6.
[9] B. Meyghani, M. Awang, C.S. Wu, Finite element modeling of friction stir welding (FSW) on a complex curved plate, J. Adv. Join. Process. 1 (2020) 100007. https://doi.org/10.1016/j.jajp.2020.100007.
[10] R. Bhattacharjee, P. Biswas, Review on thermo-mechanical and material flow analysis of dissimilar friction stir welding, Weld. Int. 35 (2021) 295–332. https://doi.org/10.1080/09507116.2021.1992256.
[11] Z. Han, L. Cao, Research progress on numerical simulation of temperature field in friction stir welding of dissimilar alloys, in: 2022 2nd Int. Conf. Algorithms High Perform. Comput. Artif. Intell. Ahpcai 2022, 2022: pp. 290–296. https://doi.org/10.1109/AHPCAI57455.2022.10087392.
[12] C. Wu, H. Su, L. Shi, Numerical Simulation of Heat Generation, Heat Transfer and Material Flow in Friction Stir-Welding, Jinshu Xuebao Acta Metall. Sin. 54 (2018) 265–277. https://doi.org/10.11900/0412.1961.2017.00294.
[13] E. Mirkoohi, D.E. Sievers, H. Garmestani, S.Y. Liang, Thermo-mechanical modeling of thermal stress in metal additive manufacturing considering elastoplastic hardening, CIRP J. Manuf. Sci. Technol. 28 (2020) 52–67. https://doi.org/10.1016/j.cirpj.2020.01.002.
[14] Y. Guo, Y. Ma, X. Zhang, X. Qian, J. Li, Study on residual stress distribution of 2024-T3 and 7075-T6 aluminum dissimilar friction stir welded joints, Eng. Fail. Anal. 118 (2020). https://doi.org/10.1016/j.engfailanal.2020.104911.
[15] M. Reza-E-Rabby, K. Ross, M. McDonnell, S.A. Whalen, Numerical simulation and experimental validation of joint performance in aluminum-steel lap welds formed by friction stir dovetailing, J. Mater. Process. Technol. 277 (2020). https://doi.org/10.1016/j.jmatprotec.2019.116459.
[16] L. Wang, C.M. Davies, R.C. Wimpory, L.Y. Xie, K.M. Nikbin, Measurement and simulation of temperature and residual stress distributions from friction stir welding AA2024 Al alloy, Mater. High Temp. 27 (2010) 167–178. https://doi.org/10.3184/096034010X12813743510192.
[17] P.K. Muhuri, A.K. Shukla, A. Abraham, Industry 4.0: A bibliometric analysis and detailed overview, Eng. Appl. Artif. Intell. 78 (2019) 218–235. https://doi.org/10.1016/j.engappai.2018.11.007.
[18] A. Simar, Y. Bréchet, B. de Meester, A. Denquin, C. Gallais, T. Pardoen, Integrated modeling of friction stir welding of 6xxx series Al alloys: Process, microstructure and properties, Prog. Mater. Sci. 57 (2012) 95–183. https://doi.org/10.1016/j.pmatsci.2011.05.003.
[19] S. Bag, D. Yaduwanshi, S. Pal, Heat transfer and material flow in friction stir welding, 2014. https://doi.org/10.1533/9780857094551.21.
[20] M. Akbari, M.R.M. Aliha, F. Berto, Investigating the role of different components of friction stir welding tools on the generated heat and strain, Forces Mech. 10 (2023) 100166. https://doi.org/10.1016/j.finmec.2023.100166.
[21] X. Zhang, L. Shi, C. Wu, C. Yang, S. Gao, Multi-phase modelling of heat and mass transfer during Ti/Al dissimilar friction stir welding process, J. Manuf. Process. 94 (2023) 240–254. https://doi.org/10.1016/j.jmapro.2023.03.037.
[22] T. Kasirajan, M. Selva Kumar, T. Ramkumar, M. Mohanraj, Thermal and mechanical characterisation of friction stir welded dissimilar aluminium alloys, Proc. Inst. Mech. Eng. Part E J. Process Mech. Eng. 239 (2025) 645–653. https://doi.org/10.1177/09544089241241447.
[23] S.R. R, Jagadish, C. Rao, S. Kumar Aadapa, S. Yanda, Predication of temperature distribution and strain during FSW of dissimilar Aluminum alloys using Deform 3D, Mater. Today Proc. 59 (2022) 1760–1767. https://doi.org/10.1016/j.matpr.2022.04.371.
[24] Y.H. Jin, Z.Y. Huang, C.F. Li, Interface characterization and materials flow pattern analysis for friction stir welding overlap joints of Mg/Al dissimilar alloys, 2014. https://doi.org/10.4028/www.scientific.net/AMM.624.106.
[25] X. Wang, D.A. Lados, Understanding the Material Flow Mechanisms—Microstructure Evolution—Defect Formation Relationships and Effects on Mechanical Properties in Friction Stir Welding of Dissimilar Aluminum Alloys, Metall. Mater. Trans. Phys. Metall. Mater. Sci. 54 (2023) 727–744. https://doi.org/10.1007/s11661-022-06921-w.
[26] X. Zhang, L. Shi, C. Wu, C. Yang, S. Gao, Multi-phase modelling of heat and mass transfer during Ti/Al dissimilar friction stir welding process, J. Manuf. Process. 94 (2023) 240–254. https://doi.org/10.1016/j.jmapro.2023.03.037.
[27] T. Padmavathi, B.B. Naik, Influence of tool pin profile on material flow, mechanical properties and corrosion behavior of friction stir welded dissimilar Al5083-6061, Eng. Res. Express 5 (2023). https://doi.org/10.1088/2631-8695/accdb7.

[28] B. Song, Y. Zhai, D. Zuo, Y. Deng, Visualization and Numerical Simulation of Material Flow in Al/Mg Dissimilar Friction Stir Welding | Al/Mg 异种合金搅拌摩擦焊的材料流动可视化和数值模拟研究, Xiyou Jinshu Cailiao Yu Gongcheng Rare Met. Mater. Eng. 49 (2020) 1483–1490.
[29] N. Dialami, M. Cervera, M. Chiumenti, A. Segatori, Prediction of joint line remnant defect in friction stir welding, Int. J. Mech. Sci. 151 (2019) 61–69. https://doi.org/10.1016/j.ijmecsci.2018.11.012.
[30] A. Ghiasvand, M. Kazemi, M. Mahdipour Jalilian, H. Ahmadi Rashid, Effects of tool offset, pin offset, and alloys position on maximum temperature in dissimilar FSW of AA6061 and AA5086, Int. J. Mech. Mater. Eng. 15 (2020). https://doi.org/10.1186/s40712-020-00118-y.
[31] R. Anbukkarasi, S.V. Kailas, Influences of shape of the new interfaces and morphology of the intermetallics on mechanical properties of aluminum AA2024–pure copper joints by friction stir welding, Int. J. Adv. Manuf. Technol. 106 (2020) 5071–5083. https://doi.org/10.1007/s00170-019-04911-8.
[32] F. Khodabakhshi, M. Haghshenas, J. Chen, B. Shalchi Amirkhiz, J. Li, A.P. Gerlich, Bonding mechanism and interface characterisation during dissimilar friction stir welding of an aluminium/polymer bi-material joint, Sci. Technol. Weld. Join. 22 (2017) 182–190. https://doi.org/10.1080/13621718.2016.1211583.
[33] W. Xue, L. Xiao, C. Huang, D. He, X. Ren, Asymmetric study on the microstructure and mechanical properties of friction stir welded joints: Finite element simulation and experiment, CIRP J. Manuf. Sci. Technol. 55 (2024) 108–128. https://doi.org/10.1016/j.cirpj.2024.09.006.
[34] H. Jamshidi Aval, Smoothed-Particle Hydrodynamics (SPH) Simulation of AA6061-AA5086 Dissimilar Friction Stir Welding, Metals 13 (2023). https://doi.org/10.3390/met13050906.
[35] G. Chen, S. Zhang, Y. Zhu, C. Yang, Q. Shi, Thermo-mechanical Analysis of Friction Stir Welding: A Review on Recent Advances, Acta Metall. Sin. Engl. Lett. 33 (2020) 3–12. https://doi.org/10.1007/s40195-019-00942-y.
[36] Y. Sharma, A. Mehta, H. Vasudev, N. Jeyaprakash, G. Prashar, C. Prakash, Analysis of friction stir welds using numerical modelling approach: a comprehensive review, Int. J. Interact. Des. Manuf. 18 (2024) 5329–5342. https://doi.org/10.1007/s12008-023-01324-6.
[37] S. Banerjee, P.C. Roy, Material Flow and Heat Transfer Analysis in Friction Stir Welding, 2025. https://doi.org/10.1002/9781394331925.ch5.
[38] M.D. Parre, T. Krishna Murthy, K. Lanka, V.K. Pasam, Numerical Simulation of Friction Stir Welding Process to Investigate the Material Flow in AA7020, 2023. https://doi.org/10.1007/978-981-19-2188-9_16.
[39] M. Chiumenti, M. Cervera, C. Agelet de Saracibar, N. Dialami, Numerical modeling of friction stir welding processes, Comput. Methods Appl. Mech. Eng. 254 (2013) 353–369. https://doi.org/10.1016/j.cma.2012.09.013.
[40] G. Buffa, L. Fratini, R. Shivpuri, CDRX modelling in friction stir welding of AA7075-T6 aluminum alloy: Analytical approaches, J. Mater. Process. Technol. 191 (2007) 356–359. https://doi.org/10.1016/j.jmatprotec.2007.03.033.
[41] M. Assidi, L. Fourment, S. Guerdoux, T. Nelson, Friction model for friction stir welding process simulation: Calibrations from welding experiments, Int. J. Mach. Tools Manuf. 50 (2010) 143–155. https://doi.org/10.1016/j.ijmachtools.2009.11.008.
[42] K. Brooks, B. Ramos, D.J. Prymak, T.W. Nelson, M.P. Miles, Improving Simulation Model Accuracy for Friction Stir Welding of AA 2219, Materials 18 (2025). https://doi.org/10.3390/ma18051046.
[43] M.D. Parre, T. Krishna Murthy, K. Lanka, P. Vamsi Krishna, Numerical Simulation for Predicting the Temperature Distribution in Friction Stir Welding of AA7020, Int. J. Veh. Struct. Syst. 13 (2021) 634–638. https://doi.org/10.4273/ijvss.13.5.16.
[44] D. Micallef, D. Camilleri, P. Mollicone, Simplified thermo-elastoplastic numerical modelling techniques applied to friction stir welding of mild steel, in: ASME Int. Mech. Eng. Congr. Expo. Proc. Imece, 2013. https://doi.org/10.1115/IMECE2013-64387.
[45] C. Wu, H. Su, L. Shi, Numerical Simulation of Heat Generation, Heat Transfer and Material Flow in Friction Stir-Welding, Jinshu Xuebao Acta Metall. Sin. 54 (2018) 265–277. https://doi.org/10.11900/0412.1961.2017.00294.
[46] R. Soto-Diaz, M. Vásquez-Carbonell, J. Escorcia-Gutierrez, A review of artificial intelligence techniques for optimizing friction stir welding processes and predicting mechanical properties, Eng. Sci. Technol. Int. J. 62 (2025). https://doi.org/10.1016/j.jestch.2025.101949.
[47] R.M. Lenka, P. More, T.A. Wani, U. Bobamuratov, M.I.R. Ugli, T. Phadtare, A. Dauletov, S. Rane, Reinforcement learning-based real-time optimization of friction stir welding parameters for copper–aluminium dissimilar interfaces, Mater. Today Commun. 52 (2026). https://doi.org/10.1016/j.mtcomm.2026.114982.
[48] R.D. Nazarlou, R. Pathak, O. Schmidt, C. Köpp, E. Münchinger, C. Schilling, S. Salim, M. Wiegand, M. Kahlmeyer, Y. Jiang, Y. Jiang, S. Böhm, Optimizing and development of friction stir welding using AI-supported prediction method and digital twin technology, Weld. World (2025). https://doi.org/10.1007/s40194-025-02245-6.
[49] B. Meyghani, M.B. Awang, S.S. Emamian, M.K.B. Mohd Nor, S.R. Pedapati, A comparison of different finite element methods in the thermal analysis of friction stir welding (FSW), Metals 7 (2017). https://doi.org/10.3390/met7100450.

[50] R.M. Bagadi, J. Jaidi, G.M. Karthik, S.D. Meshram, Arbitrary-Lagrangian-Eulerian Model Predictions and Experimental Investigations on Friction Stir Welding of Thick AA2219-T87 Plates, J. Mater. Eng. Perform. 35 (2026) 13756–13770. https://doi.org/10.1007/s11665-025-12591-7.
[51] C.A. De Saracibar, M. Chiumenti, D. Santiago, M. Cervera, N. Dialami, G. Lombera, A computational model for the numerical simulation of FSW processes, in: Aip Conf. Proc., 2010: pp. 81–88. https://doi.org/10.1063/1.3457640.
[52] M. Boukraa, T. Chekifi, S. Adjel, L. Beghdadi, A. Chibani, D. Belfennache, Friction stir welding: a review-driven exploration of simulation and optimization techniques, Weld. Int. 39 (2025) 539–558. https://doi.org/10.1080/09507116.2025.2516044.
[53] Z. Zhu, M. Wang, H.-J. Zhang, X. Zhang, T. Yu, Z.-Q. Wu, Simulation on material flow and defect during friction stir welding based on CEL method | 基于 CEL 方法搅拌摩擦焊材料流动及缺陷的模拟, Zhongguo Youse Jinshu Xuebao Chin. J. Nonferrous Met. 28 (2018) 294–299. https://doi.org/10.19476/j.ysxb.1004.0609.2018.02.10.
[54] K.N. Salloomi, Defect monitoring in dissimilar friction stir welding of aluminum alloys using Coupled Eulerian-Lagrangian (CEL) finite element model, Adv. Mater. Process. Technol. 9 (2022) 931–947. https://doi.org/10.1080/2374068X.2022.2106669.
[55] M. Akbari, H. Rahimi Asiabaraki, E. Hassanzadeh, M. Esfandiar, Simulation of dissimilar friction stir welding of AA7075 and AA5083 aluminium alloys using Coupled Eulerian–Lagrangian approach, Weld. Int. 37 (2023) 174–184. https://doi.org/10.1080/09507116.2023.2205035.
[56] R.V. Marode, M. Awang, V.S.R. Janga, Computational Modelling and Comparative Analysis of Friction Stir Welding and Stationary Shoulder Friction Stir Welding on AA6061, Crystals 13 (2023). https://doi.org/10.3390/cryst13091317.
[57] E. Shishova, F. Panzer, M. Werz, P. Eberhard, Reversible inter-particle bonding in SPH for improved simulation of friction stir welding, Comput. Part. Mech. 10 (2023) 555–564. https://doi.org/10.1007/s40571-022-00510-9.
[58] S.W. Kang, B.S. Jang, A study on computational fluid dynamics simulation of friction stir welding, in: Anal. Des. Mar. Struct. Proc. 4th Int. Conf. Mar. Struct. Marstruct 2013, 2013: pp. 433–439. https://doi.org/10.1201/b15120-59.
[59] G. Chen, Q. Shi, S. Zhang, Recent development and applications of CFD simulation for friction stir welding, 2018. https://doi.org/10.1007/978-3-319-72059-3_11.
[60] G.T. Alvali, Y. Sarikavak, Effect of tool rotation speed on thermo-mechanical behavior in dissimilar FSW of 304L stainless steel and Ti–6Al–4V: a FEM-based approach, J. Braz. Soc. Mech. Sci. Eng. 48 (2026). https://doi.org/10.1007/s40430-025-06138-z.
[61] J. Abhilash, Apeksha, B. Acharjee, Simulation of friction stir welding using thermo-mechanical coupled finite element method, in: Iop Conf. Ser. Mater. Sci. Eng., 2018. https://doi.org/10.1088/1757-899X/455/1/012113.
[62] D. Myung, W. Noh, J.-H. Kim, J. Kong, S.-T. Hong, M.-G. Lee, Probing the Mechanism of Friction Stir Welding with ALE Based Finite Element Simulations and Its Application to Strength Prediction of Welded Aluminum, Met. Mater. Int. 27 (2021) 650–666. https://doi.org/10.1007/s12540-020-00901-8.
[63] N. Hannachi, A. Khalfallah, C. Leitão, D.M. Rodrigues, Comparison Between ALE and CEL Finite Element Formulations to Simulate Friction Stir Spot Welding, 2022. https://doi.org/10.1007/978-3-030-86446-0_36.
[64] Y. Su, H. Xia, S. Chen, C. Wang, S. Wu, W. Lu, J. Zhu, H. Wu, Thermo-mechanical-fluid coupled modeling for residual stress prediction in thick plate welding, J. Mater. Res. Technol. 36 (2025) 7557–7571. https://doi.org/10.1016/j.jmrt.2025.04.323.
[65] Z. Sarfaraz, Y.R. Awan, H.A. Saeed, R. Khan, M. Wieczorowski, N.A. Din, Residual Stress in Friction Stir Welding of Dissimilar Aluminum Alloys: A Parametric Study, Materials 18 (2025) 316. https://doi.org/10.3390/ma18020316.
[66] A.I. Hosny, J. Sheikh-Ahmad, F. Almaskari, K. Khan, S. Deveci, A.I. Alhatti, Effect of process temperatures on joining aluminum alloy (AA5052) to polypropylene (PP) by friction lap welding, J. Mater. Res. Technol. 33 (2024) 5277–5288. https://doi.org/10.1016/j.jmrt.2024.10.107.
[67] N.T. Yousef, R. Yousef, Digital Twin-Enabled Predictive Analytics for Friction Stir Welding: Multi-Physics Simulation, Sensor Synchronization, and Defect Detection, (2026). https://doi.org/10.21203/rs.3.rs-8702698/v1.
[68] J.Y. Sheikh-Ahmad, D.S. Ali, S. Deveci, F. Almaskari, F. Jarrar, Friction stir welding of high density polyethylene—Carbon black composite, J. Mater. Process. Technol. 264 (2019) 402–413. https://doi.org/10.1016/j.jmatprotec.2018.09.033.